JCI insight

Myocardial fibrosis after adrenergic stimulation as a long-term sequela in a mouse model of Kawasaki disease vasculitis

Harry H. Matundan, … , Masanori Abe, Moshe Arditi

JCI Insight. 2019;4(3):e126279. https://doi.org/10.1172/jci.insight.126279.

Research Article **Cardiology** **Vascular biology**

Kawasaki disease (KD), the leading cause of acquired cardiac disease among children, is often associated with myocarditis that may lead to long-term myocardial dysfunction and fibrosis. Although those myocardial changes develop during the acute phase, they may persist for decades and closely correlate with long-term myocardial sequelae. Using the *Lactobacillus casei* cell wall extract–induced (LCWE-induced) KD vasculitis murine model, we investigated long-term cardiovascular sequelae, such as myocardial dysfunction, fibrosis, and coronary microvascular lesions following adrenergic stimuli after established KD vasculitis. We found that adrenergic stimulation with isoproterenol following LCWE-induced KD vasculitis in mice was associated with increased risk of cardiac hypertrophy and myocardial fibrosis, diminished ejection fraction, and increased serum levels of brain natriuretic peptide. Myocardial fibrosis resulting from pharmacologic-induced exercise after KD development was IL-1 signaling dependent and was associated with a significant reduction in myocardial capillary CD31 expression, indicative of a rarefied myocardial capillary bed. These observations suggest that adrenergic stimulation after KD vasculitis may lead to cardiac hypertrophy and bridging fibrosis in the myocardium in the LCWE-induced KD vasculitis mouse model and that this process involves IL-1 signaling and diminished microvascular circulation in the myocardium.

JCI insight

RESEARCH ARTICLE

Myocardial fibrosis after adrenergic stimulation as a long-term sequela in a mouse model of Kawasaki disease vasculitis

Harry H. Matundan,[1] Jon Sin,[2] Magali Noval Rivas,[1,3,4] Michael C. Fishbein,[5] Thomas J. Lehman,[6] Shuang Chen,[1,3,4] Roberta A. Gottlieb,[2] Timothy R. Crother,[1,3,4] Masanori Abe,[1] and Moshe Arditi[1,2,3,4]

[1]Departments of Biomedical Sciences and Pediatrics, Divisions of Infectious Diseases and Immunology, [2]Cedars-Sinai Heart Institute, Barbra Streisand Women's Heart Center, and [3]Infectious and Immunologic Diseases Research Center, Cedars-Sinai Medical Center, Los Angeles, California, USA. [4]Department of Pediatrics and [5]Department of Pathology, David Geffen School of Medicine at UCLA, Los Angeles, California, USA. [6]Pediatric Rheumatology, Hospital for Special Surgery and Weill Medical College of Cornell University, New York, New York, USA.

Kawasaki disease (KD), the leading cause of acquired cardiac disease among children, is often associated with myocarditis that may lead to long-term myocardial dysfunction and fibrosis. Although those myocardial changes develop during the acute phase, they may persist for decades and closely correlate with long-term myocardial sequelae. Using the *Lactobacillus casei* cell wall extract–induced (LCWE-induced) KD vasculitis murine model, we investigated long-term cardiovascular sequelae, such as myocardial dysfunction, fibrosis, and coronary microvascular lesions following adrenergic stimuli after established KD vasculitis. We found that adrenergic stimulation with isoproterenol following LCWE-induced KD vasculitis in mice was associated with increased risk of cardiac hypertrophy and myocardial fibrosis, diminished ejection fraction, and increased serum levels of brain natriuretic peptide. Myocardial fibrosis resulting from pharmacologic-induced exercise after KD development was IL-1 signaling dependent and was associated with a significant reduction in myocardial capillary CD31 expression, indicative of a rarefied myocardial capillary bed. These observations suggest that adrenergic stimulation after KD vasculitis may lead to cardiac hypertrophy and bridging fibrosis in the myocardium in the LCWE-induced KD vasculitis mouse model and that this process involves IL-1 signaling and diminished microvascular circulation in the myocardium.

Introduction

Kawasaki disease (KD) is an acute febrile illness and systemic vasculitis of unknown etiology that predominantly afflicts young children and causes coronary artery aneurysms (CAAs) or abnormalities that can ultimately lead to ischemic heart disease, myocardial infarction, and even death (1–7). KD is the leading cause of acquired heart disease among children in the USA and developed countries (3). CAAs occur in about 30% of untreated pediatric patients, but this rate is reduced to 5% with high-dose intravenous immunoglobulin (IVIG) treatment (8, 9). However, IVIG resistance has increased over recent years, and approximately 20% of KD patients are IVIG resistant and thus at higher risk of developing CAAs (8–11).

Acute KD vasculitis was initially thought to be a self-limited disease; however, increasing observations now reveal that chronic cardiovascular remodeling persists after the acute phase and can progress into adulthood (12, 13). This has led to a recent shift in research interests and increased focus on the presence of chronic, long-term cardiovascular sequelae following KD vasculitis. Indeed, scientific reports increasingly indicate that patients with KD history are at higher risk of cardiovascular complications beyond childhood (7, 14–17).

Although most attention in KD research and clinical practice has focused on the development of CAAs during acute KD, and on long-term complications of coronary artery stenosis and ischemia (18, 19), KD-induced myocarditis is more prevalent than CAAs (20–24). Histologic features of myocarditis are found in all KD patients during the acute phase, irrespective of the presence of CAAs (25–28), and myocarditis is also

Authorship note: HHM and JS contributed equally to this work. M. Abe and M. Arditi contributed equally to this work.

Conflict of interest: The authors have declared that no conflict of interest exists.

Submitted: November 19, 2018
Accepted: January 3, 2019
Published: February 7, 2019

Reference information:
JCI Insight. 2019;4(3):e126279.
https://doi.org/10.1172/jci.insight.126279.

a cause of death in early fatal KD cases (29, 30). Myocarditis is subclinical in the majority of KD patients, and those who are symptomatic may present with mild clinical, electrocardiographic or echocardiographic signs of ventricular dysfunction. Occasionally children present with KD shock syndrome and hemodynamic instability as a result of decreased systolic function and vasoplegia (26). In many children with KD, echocardiograph shows depressed shortening fraction, and increased end-systolic and end-diastolic dimension strain abnormalities and diastolic dysfunction are also found in a significant proportion of patients (31, 32). While most studies report improvement of myocardial function with treatment, there is now growing evidence that ongoing myocardial abnormalities occur in the long term (24). It has recently been shown that children suffering from subclinical myocardial complications during acute KD display long-term cardiovascular complications, such as lower myocardial flow reserve and higher total coronary resistance (33–35). However, few studies have considered a potential link between myocarditis in childhood KD and long-term persistent damage to the myocardium, including myocardial remodeling and fibrosis (30, 36).

Whether the myocarditis that occurs with the acute illness leads to long-term pathology, such as fibrosis and myocyte dropout, independent of coronary artery abnormalities is not clear. There have been several reported cases in which adolescents or young adults who had childhood KD vasculitis but no known previous cardiovascular history presented with angina, myocardial infarction, ischemia-induced arrhythmia, sudden death, or myocardial fibrosis (4, 5). Increasing numbers of deaths attributable to left ventricular dysfunction and presumed ventricular arrhythmias are being reported in young adults from Japan with antecedent KD (37). Some autopsy reports of adults long after KD describe cardiomyocyte dropout and diffuse fibrosis occurring outside the watershed distribution of the epicardial coronary arteries (5). Therefore, whether the diffuse myocardial fibrosis described in these cases is a consequence of ischemic injury from microinfarcts, inflammatory injury to cardiomyocytes from initial myocarditis, or both is unknown.

A murine model of coronary arteritis is available that closely phenocopies the important histological and immune pathological features of the cardiovascular lesions seen in human KD vasculitis (i.e., coronary arteritis, coronary stenosis, aortitis, myocarditis, and aneurysms) (38–40). This widely used murine model relies on a single i.p. injection of *Lactobacillus casei* cell wall extract (LCWE) to elicit self-reactive immune responses and histopathological features of the cardiovascular lesions similar to human KD pathology (38–40). These include coronary arteritis, aortitis, and aneurysms as well as myocarditis. Here, we used the LCWE murine model of KD vasculitis to investigate the long-term cardiovascular complications following acute KD vasculitis. We observed that, following the initial acute KD vasculitis and a recovery period, mice that undergo β-adrenergic stimulant isoproterenol (ISO) stimulation (as a pharmacological model of exercise or stress) develop significant cardiac hypertrophy, bridging fibrosis in the myocardium, and scarring as well as decreased myocardial function. The pathological mechanisms involved in this late cardiovascular complication following acute KD may involve capillary endothelial cell loss in the myocardium following acute KD vasculitis and adrenergic stimuli. In addition, IL-1 receptor–deficient (*Il1r1*$^{-/-}$) mice were protected from developing late myocardial fibrosis, indicating that this process requires IL-1 signaling.

Results

LCWE-induced KD vasculitis predisposes to adrenergic stress-induced myocardial fibrosis and myocardial dysfunction. Though the acute symptoms of KD are well-characterized, the lasting myocardial alterations following the resolution of the initial inflammation are unclear. To investigate the chronic phase of the disease, we employed the LCWE-induced murine model of KD, wherein WT, 5-week-old mice are treated with LCWE. Five weeks following LCWE treatment, at which point there was no observable remnant myocardial inflammation, as determined by H&E staining (Supplemental Figure 1; supplemental material available online with this article; https://doi.org/10.1172/jci.insight.126279DS1), mice were treated with the β-agonist ISO for 10 days to elicit cardiac stress (Figure 1A). Hearts from mice that did not receive ISO were not hypertrophic, regardless of previous LCWE injection (Figure 1B), and LCWE injection did not result in significant differences in the ratio of heart weight to tibia length (HW/TL) in these groups (Figure 1C). Additionally, no sign of myocardial scarring could be observed in vehicle-treated PBS- or LCWE-injected mice (Figure 1, D and E). As expected, ISO treatment induced a significant increase in HW/TL in naive mice; however, fibrosis was not consistently observed in this group (Figure 1, B–D). In contrast, hearts from ISO-treated LCWE-injected mice exhibited exaggerated hypertrophy and were profoundly fibrotic (Figure 1, B–E).

Natriuretic peptides, such as B-type natriuretic peptide (BNP), are secreted from the myocardium in the presence of increased intracardiac pressure and myocardial stress (41). Serum levels of BNP were mod-

estly increased in ISO-treated PBS control mice; however, this was dramatically elevated in ISO-treated LCWE-injected KD mice (Figure 1F). Additionally, MRI on these animals showed significantly reduced ejection fractions in LCWE-injected KD mice given ISO (Figure 1G). This functional impairment was not observed in vehicle-treated LCWE-injected mice. These results reveal that, even after acute LCWE-induced KD myocardial inflammation has resolved, mice are significantly more susceptible to stress-induced impairments in myocardial function.

IL-1 signaling is required for adrenergic stress-induced myocardial fibrosis following murine KD vasculitis. We have previously demonstrated that IL-1β is involved in the development of coronary lesions at the aortic root during the acute phase of KD (38, 39, 42). We next tested if impaired IL-1 signaling would reduce pathological cardiac remodeling in ISO-treated LCWE-injected mice. *Il1r1*$^{-/-}$ mice were injected with LCWE to induce KD vasculitis, and 5 weeks later they were treated with ISO. Compared with LCWE-injected WT mice, heart hypertrophy was significantly blunted in *Il1r1*$^{-/-}$ mice after ISO treatment (Figure 2, A and B). Consistent with this, Masson's trichrome staining showed a dramatic reduction in myocardial fibrosis in the *Il1r1*$^{-/-}$ mice (Figure 2, C and D). Additionally, unlike WT mice, *Il1r1*$^{-/-}$ mice treated with ISO displayed no significant reduction in ejection fraction by MRI (Figure 2E). These findings reveal the central role of IL-1 signaling in the progression of pathological cardiac remodeling, such as the late development of bridging fibrosis in the myocardium and deterioration of myocardial function, and highlight the IL-1 pathway as a potential therapeutic target in the treatment of KD-related acute and long-term cardiac sequelae.

The acute effect of KD vasculitis on myocardial capillary endothelial cell density is amplified by adrenergic stress. In a previous study, our group showed that a low-grade subclinical infection with coxsackie virus B3 in mice during the neonatal phase caused sensitization to stress-induced dilated cardiomyopathy during adulthood, related to reduced levels of the angiogenic protein VEGF (43). Additionally, infected mice showed an inability to increase capillary density to compensate for the ISO-induced increase in cardiac load. Given the finding that, in the asymptomatic KD chronic phase, the heart is also more sensitive to adrenergic insults, we next investigated the potential that structural alterations stemmed from the initial KD insult. Immunohistochemistry revealed a significant reduction in myocardial expression of the endothelial cell marker CD31 after LCWE-induced KD vasculitis, which was further enhanced following ISO treatment 5 weeks after induction of KD vasculitis (Figure 3, A and B). As above, *IL1r1*$^{-/-}$ mice were protected from this effect (Figure 3, A and B). Western blots of heart homogenates showed a significant reduction in VEGF protein in WT LCWE-injected KD mice (Figure 3, C and D). Taken together, these data indicate that LCWE-induced vasculitis not only results in rarefied cardiac capillary networks, but also reduces angiogenic potential due to diminished VEGF expression. This setting of impaired vascular remodeling capacity could leave the heart more susceptible to damage during physiological stress, as the cardiac muscle would be unable to compensate for the oxygen demand that accompanies increased cardiac load.

Increased myocardial macrophage infiltration in areas of myocardial fibrosis in LCWE-injected KD mice following ISO treatment. Ischemic injury in the heart induces an inflammatory cascade, and infiltrating macrophages are known to both repair injury and exacerbate myocardial scarring and fibrosis formation in the damaged heart (44, 45). To investigate whether the ISO-induced myocardial fibrosis after KD was associated with macrophage recruitment in the hearts of the LCWE-injected mice, we stained heart sections for the macrophage/monocyte marker MOMA-2. Macrophage recruitment was markedly increased in areas of myocardial fibrosis in the KD vasculitis group following ISO treatment compared with that in naive mice (no KD vasculitis) that received ISO injections (Figure 4 and Supplemental Figure 2).

Discussion

Multiple cardiovascular sequelae have been reported after acute KD, especially in patients with coronary artery lesions (24). Although CAAs can remodel in 50%–80% of cases depending on the age of onset, all patients with aneurysms are at risk for ischemic heart disease due to thrombosis or stenosis of the affected coronary arteries (21, 46). Therefore, it is now increasingly recognized that KD is not a self-limited disease and that it can result in late and long-lasting cardiovascular complications, such as coronary artery stenosis, valve impairment, ischemic heart disease, and myocardial fibrosis. In addition, CAAs may remain silent and persist into adulthood when myocardial ischemia can lead to sudden death (5, 47).

The development of myocarditis during the acute phase of KD is a universal histologic finding present in all patients, can occur in the absence of coronary artery abnormalities, and is more prevalent than CAAs (27, 48–52). The presence of myocarditis in the acute phase is supported by pathology, biopsy, nuclear

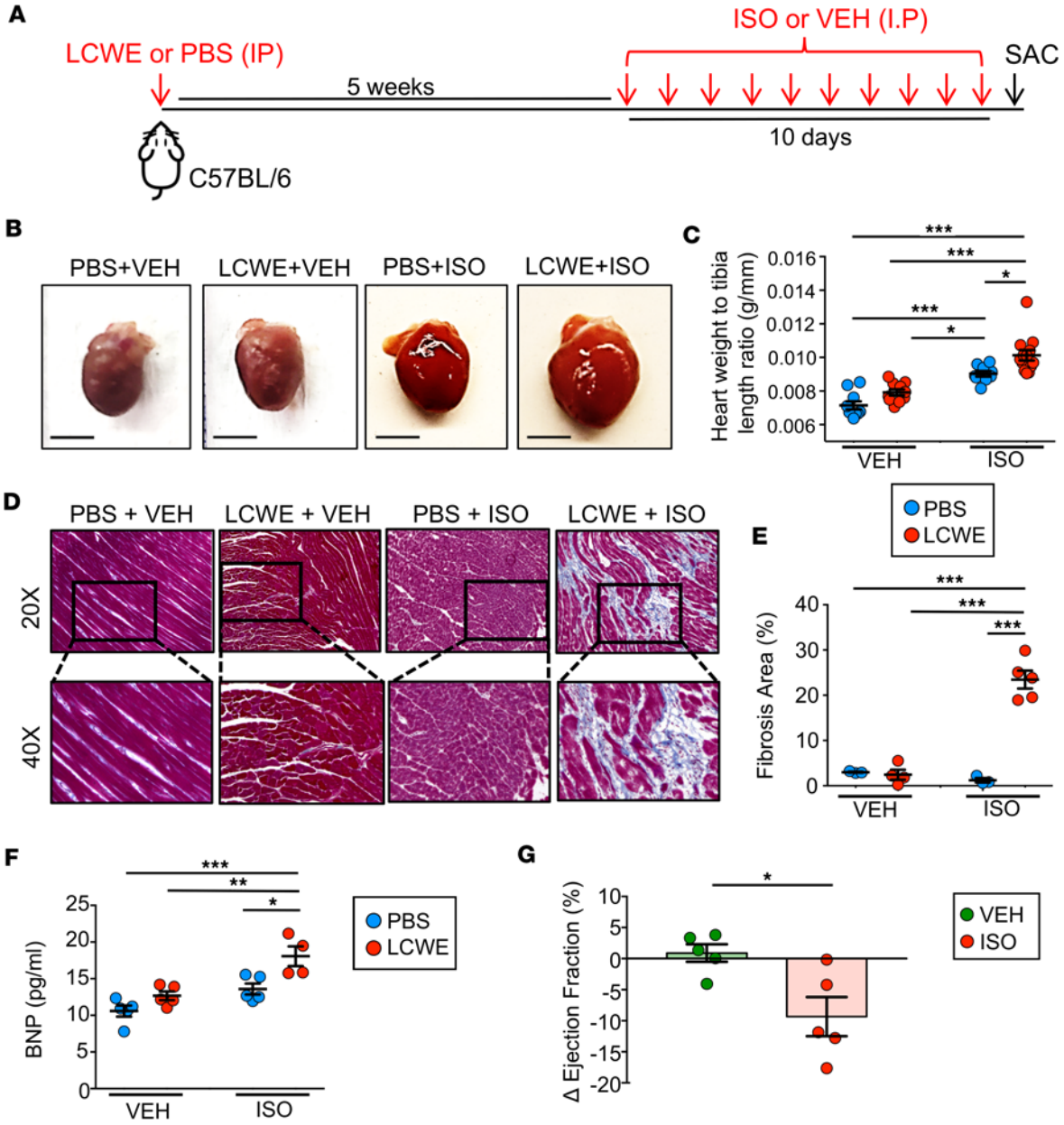

Figure 1. Pharmacologic stress induces myocardial fibrosis and myocardial dysfunction in LCWE-injected WT mice. (**A**) Schematic representation of the experimental set up. WT mice were injected with LCWE or PBS and 5 weeks later received daily either ISO or an equal volume of VEH sesame oil for 10 consecutive days. Twenty-four hours after the last ISO or VEH injection, sera and heart tissues were collected to evaluate the pathology. (**B**) Representative images of heart tissues collected from PBS-injected mice treated with VEH, LCWE-injected mice treated with VEH, PBS-injected mice treated with ISO, and LCWE-injected mice treated with ISO. Scale bars: 5 mm. (**C**) Heart-weight-to-tibia-length measurements of hearts from each of the mouse groups in **B**. (**D**) Representative images of heart sections of the mouse group in **B** stained with Masson's trichrome (original magnification, ×20 [top]; ×40 [bottom]). (**E**) Quantification of myocardial fibrosis, as determined by Masson's trichrome staining presented as percentage of blue area (collagen) of total area analyzed. (**F**) BNP levels in blood taken from LCWE-injected WT mice following VEH or ISO treatment. (**G**) Differences in ejection fractions (EF) of LCWE-injected WT mice before and after VEH or ISO treatment, as measured by MRI. EF was measured before and after ISO treatment. $\Delta EF = EF_{after} - EF_{before}$. Data are presented as mean ± SEM. $^{*}P < 0.05$, $^{**}P < 0.01$, $^{***}P < 0.001$ by 2-way ANOVA or Mann Whitney *t* test, 4–14 mice per group. LCWE, *Lactobacillus casei* cell wall extract; ISO, isoproterenol; VEH, vehicle.

imaging, echocardiography, magnetic resonance, and serum biomarker studies. A systematic study of 29 KD patients who died within the first 40 days after fever onset demonstrated myocarditis with varying degrees of infiltration of inflammatory cells in all cases (28). While most KD patients exhibit subclinical myocarditis, it is also a cause of death in some cases (24, 29). In addition, although most studies report

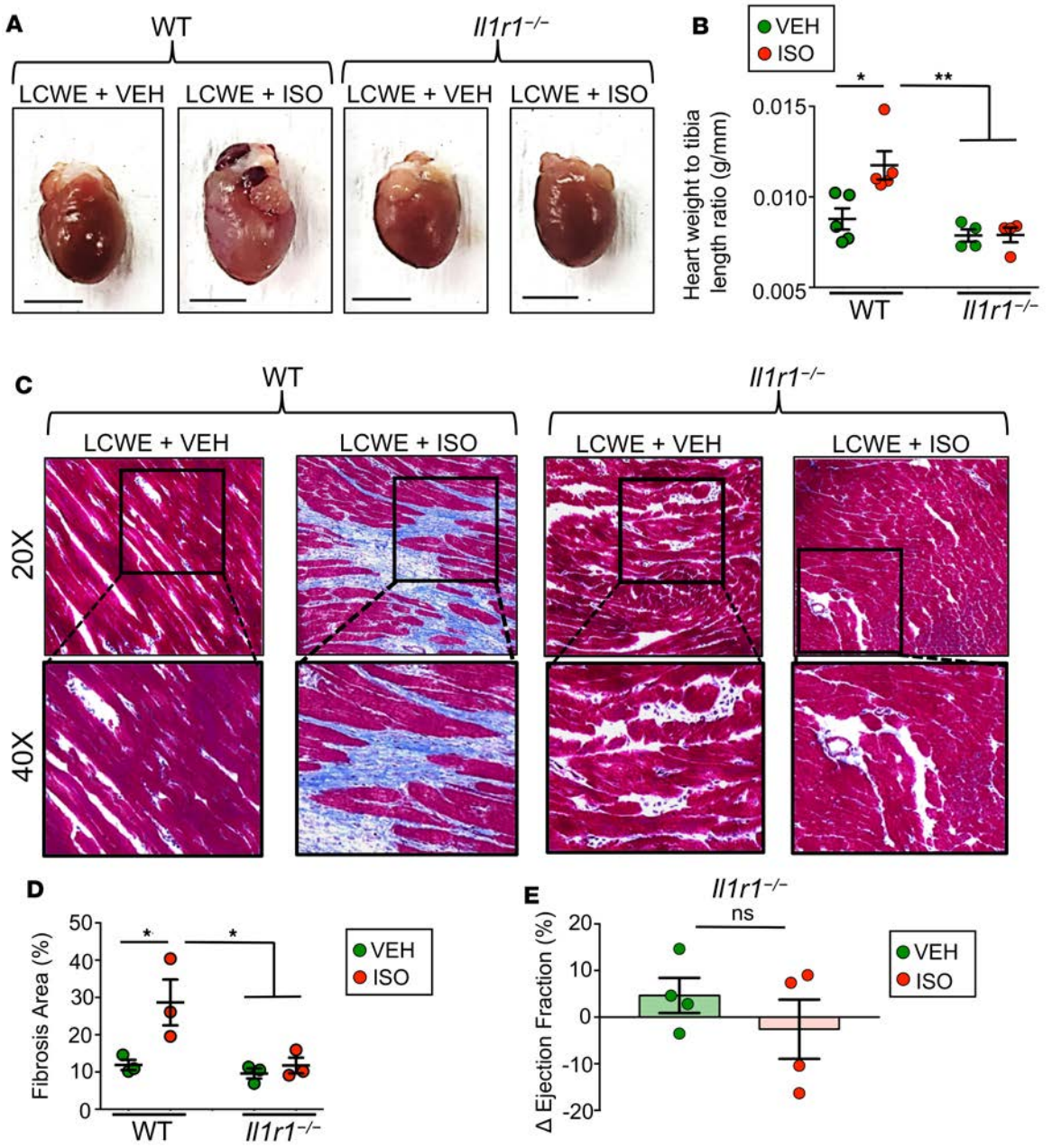

Figure 2. ISO-induced myocardial fibrosis is IL-1 dependent. WT or *Il1r1*$^{-/-}$ mice were either injected with PBS or LCWE to induce KD vasculitis and allowed to recover for 5 weeks before receiving either ISO or VEH daily for 10 consecutive days. Twenty-four hours after the last ISO or VEH injection, heart tissues were collected. (**A**) Representative images of heart tissues collected from WT and *Il1r1*$^{-/-}$ mice injected with PBS or LCWE and treated with ISO or VEH. Scale bars: 5 mm. (**B**) Heart-weight-to-tibia-length measurements of hearts collected from the different treatment groups. (**C**) Representative images of heart sections stained via Masson's trichrome (original magnification, ×20 [top]; ×40 [bottom]). (**D**) Myocardial fibrosis quantification, as determined by Masson's trichrome staining represented as percentage of blue area (collagen) of total area analyzed. (**E**) Differences in ejection fraction (EF) of LCWE-treated *Il1r1*$^{-/-}$ mice before and after VEH or ISO treatment, as measured by MRI. EF was measured before and after ISO treatment. $\Delta EF = EF_{after} - EF_{before}$. Data are presented as mean ± SEM. $^{*}P < 0.05$, $^{**}P < 0.001$ by 2-way ANOVA or Mann Whitney *t* test, 3–5 mice per group. LCWE, *Lactobacillus casei* cell wall extract; ISO, isoproterenol; VEH, vehicle.

improvement of myocardial function with time and after IVIG treatment, there is increasing evidence that KD myocarditis can result in ongoing myocardial pathologies and in long-term sequelae following acute KD (4, 5, 12, 53). For example, Yonesaka et al. (54) reported the presence of hypertrophy, degeneration of myocytes, and myocardial fibrosis in the majority of myocardial biopsies obtained at least 3 years after KD in 38 subjects and showed that this was more frequent in children who had experienced CAAs during the acute phase. Yutani et al. (50) found myocardial abnormalities, including lymphocyte and plasma cell

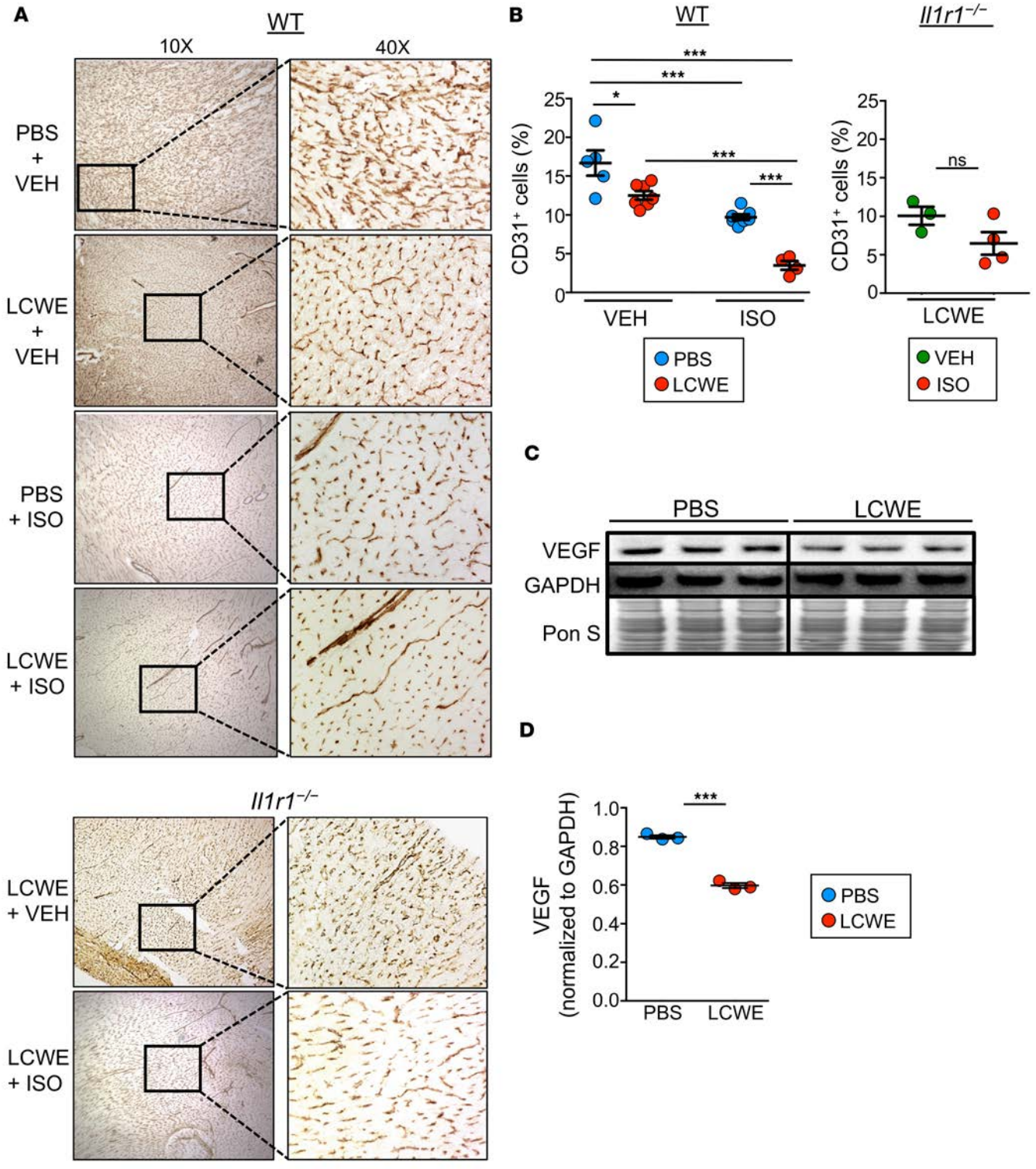

Figure 3. LCWE-induced KD vasculitis is associated with reduced myocardial capillary density. WT and *Il1r1*$^{-/-}$ mice were injected with either PBS or LCWE and allowed to recover for 5 weeks before receiving ISO or VEH daily for 10 consecutive days. Twenty-four hours after the last ISO or VEH injection, heart tissues were collected and examined. (**A**) Immunohistochemistry of CD31 expression in heart tissues of WT and *Il1r1*$^{-/-}$ mice injected either with PBS or LCWE and subsequently treated with VEH or ISO. (**B**) Quantification of CD31 staining in heart tissues from PBS- or LCWE-injected WT mice treated with ISO or VEH (left) and LCWE-injected *Il1r1*$^{-/-}$ mice treated with ISO or VEH (right). The graph represents the percentage of CD31-positive area of total area analyzed. (**C** and **D**) Western blot analysis (**C**) and quantification (**D**) of VEGF expression in heart tissue homogenates from PBS- and LCWE-injected WT mice. Data are presented as mean ± SEM. $^{*}P < 0.05$, $^{***}P < 0.001$ by 2-way ANOVA or Student's unpaired *t* test, 3–7 mice per group. LCWE, *Lactobacillus casei* cell wall extract; ISO, isoproterenol; VEH, vehicle.

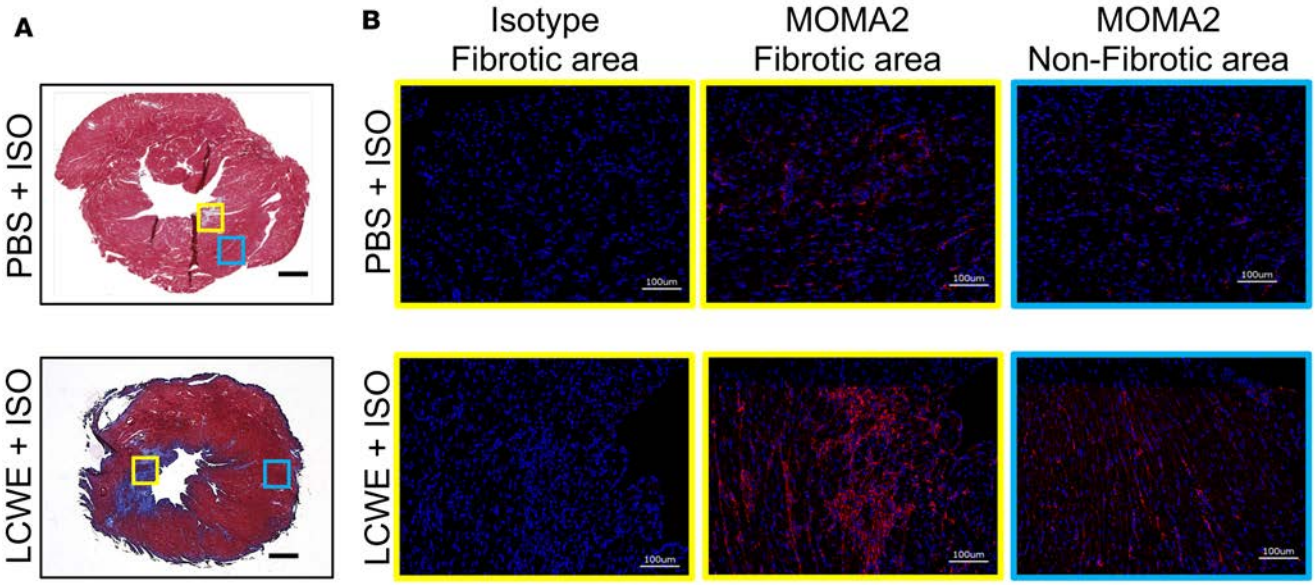

Figure 4. Increased myocardial macrophages infiltration in LCWE-induced KD vasculitis following ISO treatment. WT mice were injected with either PBS or LCWE and allowed to recover for 5 weeks before receiving ISO for 10 consecutive days. Twenty-four hours after the last ISO injection, hearts were harvested and used for histological analysis. (**A**) Representative images of Masson's trichrome–stained heart sections from PBS- or LCWE-injected KD mice treated with ISO. Scale bars: 500 μm. (**B**) MOMA2 immunofluorescent staining (red) in heart tissue fibrotic area (yellow boxes) and nonfibrotic area (blue boxes) from the mouse groups in **A**. DAPI (blue) was used to visualize nuclei. Scale bars: 100 μm. LCWE, *Lactobacillus casei* cell wall extract; ISO, isoproterenol.

infiltration, myocardial fibrosis, and disarray of myocardial fibers in every biopsy from the 201 KD patients in their study. These changes, including the myocardial fibrosis, were most pronounced patients studied 4 or more years after acute KD, raising the question of progression of myocardial pathology over time.

Here, we used the LCWE-induced murine model of KD vasculitis, which is known to recapitulate the key immunopathologic features of human KD (38–40, 42), to investigate the long-term consequences of acute KD on heart tissue. Following induction of acute experimental KD vasculitis, mice were allowed to recover for 1 month, at which point initial KD myocarditis and other cardiac parameters were completely resolved. We then mimicked exercise stress by injecting these mice with a β-adrenergic stimulant (ISO) daily for 10 days (55, 56). In mice with prior LCWE-induced vasculitis, adrenergic stimulation led to the development of myocardial fibrosis, with recruitment of macrophages to the patchy fibrotic areas, which was associated with diminished myocardial function. ISO injection alone did not elicit any fibrosis or functional alteration in hearts of naive control PBS-injected WT mice, consistent with previous studies (57).

Several studies have reported that coronary microvascular circulation can be impaired in KD patients, even in the absence of coronary artery involvement (58–60). KD patients also exhibit generalized abnormalities in endothelial cell function (61–63) and myocardial flow reserve (60, 63) that may persist for several years. However, the long-term risk and adverse effects of endothelial cell dysfunction after acute KD are controversial due to conflicting reports showing either the presence (61–63) or the absence (64–66) of long-term persistence of endothelial cells abnormalities. In line with this, a recent post hoc analysis of an international multicenter trial reported defective exercise-induced myocardial perfusion late after acute KD in 16.5%–22% of patients both with and without CAAs (67). Underscoring the impact of this effect, a recent study described 2 cases in which young adults died suddenly and unexpectedly following strenuous exercise due to sequelae of apparent KD in childhood, manifesting as giant aneurysms with thrombosis, diffuse and patchy myocardial fibrosis, and acute myocardial infarction, which was deemed the cause of death (68). Liu et al. performed an ultrastructural study on endomyocardial biopsy specimens obtained during follow-ups of 54 patients, revealing myocardial changes including hypertrophy, various degrees of cardiomyocyte degeneration, mitochondrial abnormalities, lymphocyte infiltration, and fibrosis (25). Most interestingly, they also reported microvascular abnormalities in the myocardium, such as microvascular dilatation, capillary endothelial cell injury and capillary rarefication, platelet aggregation with thrombosis, and small arteriole stenosis found in the patients up to 23 years after the convalescent stage (25). Other studies reported biopsies findings from patients who

had a prior history of KD without persistent coronary artery lesions, which revealed myocellular hypertrophy, myofibrillar disarray, and interstitial fibrosis (27, 54, 69).

In our mouse model, we observed a clear reduction of capillary endothelial cell marker CD31 expression in the myocardium of KD mice treated with vehicle control, suggestive of a rarefied capillary bed and diminished microcirculation in the myocardium following initial KD vasculitis, which was significantly exaggerated after ISO treatment. The initial loss of the myocardial capillary bed may contribute to the subsequent exacerbation of myocardial damage following sustained adrenergic stimuli. It is also possible that the perturbed microvascular architecture of the myocardium impairs perfusion during ISO-induced cardiac stress. Because myocardial oxygen demand is higher when the heart is under increased workload, cardiovascular stress may promote heart ischemia when myocardial vessel density is already reduced.

In response to myocardial infarction or ischemia, cardiac macrophages are key regulators of cardiac remodeling, providing both strong proinflammatory signals early and subsequent reparative cues later for myocardial scar formation (44, 45). Indeed, we observed that mice that developed myocardial fibrosis following acute KD vasculitis and ISO treatment also had significantly increased macrophage recruitment into the fibrotic myocardial tissue compared with naive mice treated with ISO. Additional studies are currently underway to further investigate the function and polarization of these infiltrating macrophages by analyzing their transcriptome. Future studies may be aimed at targeting specific detrimental functions of macrophages while preserving beneficial roles to prevent adverse myocardial remodeling following acute KD vasculitis.

The hearts of mice that experienced LCWE-induced KD vasculitis followed by adrenergic stimulation also exhibited classical markers of decreased myocardial function, including increased heart weight, cardiac fibrosis, and elevated serum BNP. Additionally, LCWE-injected KD mice showed significantly reduced ejection fraction following adrenergic challenge. Therefore, our results suggest that an initial insult during acute KD vasculitis and associated myocarditis may induce microscopic changes in microcirculation and endothelial cell and microcapillary damage in the myocardium, which at a much later time develops into myocardial fibrosis in the setting of sustained cardiac stress.

We also found that IL-1 signaling plays a key role in the long-term complications of acute KD vasculitis, as *Il1r1*$^{-/-}$ mice did not develop this late myocardial fibrosis and were resistant to pathological myocardial remodeling. This cardioprotection could be attributed to both a reduction in coronary arteritis and vasculitis formation during the acute phase, which is also IL-1 dependent, as we have shown previously (38, 39), as well as a blunting in hypertrophic response due to abolished IL-1β signaling, but this requires further study. Moving forward, it will be important to determine whether interventions blocking IL-1β and its receptor, in addition to inhibiting acute KD vasculitis and acute myocarditis, also limit the degree of myocardial remodeling, fibrosis and myocardial dysfunction following KD. While an IL-1R antagonist (anakinra) is now in two phase II clinical trials for IVIG-resistant KD patients (ClinicalTrials.gov NCT02179853 and NCT02390596) (70, 71), it is currently unknown how anti–IL-1 therapies will affect the long-term cardiovascular consequences of KD.

Systematic study of adolescents and adults with a history of KD in childhood is needed to define the natural history of this late myocardial fibrosis. Additional longitudinal studies, including PET imaging and magnetic resonance angiography imaging that can detect the attenuation of myocardial flow reserve, abnormal coronary flow reserve, and endothelial function, could potentially be applied to help identify the subset of KD patients with myocardial ischemia and risk for developing subsequent fibrosis. Finally, while it would be prudent to keep in mind that, although long-term clinical consequences of KD myocardial inflammation are possible, physical activity should be encouraged for all KD patients within the parameters defined by known risk factors (3) until definitive long-term clinical studies of KD patients into late adulthood are available.

Methods

Preparation of LCWE. LCWE were prepared as previously described (38). *L. casei* was grown in *Lactobacillus* de Man, Rogosa, and Sharpe broth (EMD Millipore, catalog 110661) for 48 hours, pelleted, and washed with PBS. Bacteria were disrupted with 4% SDS (MilliporeSigma, catalog 05030), and cell wall fragments were washed with PBS and sonicated in a dry ice-ethanol bath for 2 hours. Cell wall fragments were then centrifuged for 20 minutes at 20,000 *g*, the supernatant was collected and subsequently centrifuged for 1 hour at 95,000 *g* and 4°C, and the pellet was discarded. The total rhamnose content of the cell wall extract was measured by colorimetric phenol-sulfuric assay as described previously (72).

Mice and treatment protocols. Five-week-old male C57BL/6 WT mice (The Jackson Laboratory, catalog 000664) were injected i.p. with a single dose of 500 μl LCWE to induce KD vasculitis. PBS was given to

control mice. Mice were allowed to rest for 5 weeks before β-adrenergic stimulation with isoproterenol hydrochloride (ISO; MilliporeSigma, I-6504; 40 mg/kg/d). To induce cardiac stress, mice were given i.p. ISO daily for 10 days. Control mice received equivalent volumes of vehicle sesame oil (MilliporeSigma, catalog S3547). Tissues were harvested the next day following the final day of ISO or sesame oil injections. Hearts were weighed, and tibia lengths were measured to control for variations in individual growth rates of the mice and heart tissue embedded in Optimal Cutting Temperature cryoembedding compound (OCT; VWR Sakura Tissue-Tek, catalog 4583) for further histological analysis.

Histological analysis and immunostaining. Following excision, hearts were palpated in ice-cold PBS to remove residual blood and then cryoembedded in OCT. Frozen heart tissue blocks were cut into 5-μm thick sections, mounted onto charged glass microscopy slides (Fisher Scientific, catalog 1255017), and stored at –20°C. To examine myocardial inflammation, hearts were stained via hematoxylin (MilliporeSigma, catalog HHS32) and eosin (MilliporeSigma, catalog 230251). Myocardial scarring was assessed by Masson's trichrome staining (MilliporeSigma, catalog HT15-1KT). Capillary density was measured by immunostaining for endothelial marker 1:100 rabbit anti-CD31 (Abcam, catalog ab28364) and rabbit IgG as isotype control (Santa Cruz Biotechnology, catalog SC-3888). Following primary antibody labeling, sections were then incubated with 1:100 HRP-conjugated goat anti-rabbit secondary antibody (Kirkegaard & Perry Laboratories, catalog 074-1516). Sections were then dehydrated, cleared in xylene, and cover slipped using Cytoseal (VWR, 48212-187). Fibrosis quantification and CD31 positivity were performed using the Hybrid Cell Count function on a BZ-9000 Keyence microscope (Keyence). Briefly, for each stained apical heart section, 10 replicate field-of-vision images were taken at ×40 objective magnification. The Hybrid Cell Count function of the Keyence software analysis measured the percentage of CD31-positive area for each image captured and quantified the mean of all the replicate field of vision from each heart sample, which was represented as a percent area, and finally quantified the mean ± SEM for each heart sample within each group. Macrophages were stained using 1:200 rat anti-mouse MOMA-2 (Bio-Rad, catalog MCA519G) and Rat IgG2b as isotype control (Biolegend, catalog 400601). Following primary antibody labeling, sections were then incubated with 1:1000 Alexa Fluor 594–conjugated donkey anti-rat secondary antibody (Thermo Fisher Scientific, catalog A-21209). Sections were then cover slipped in ProLong Gold Antifade mounting medium with DAPI (Thermo Fisher Scientific, catalog P36931). Stained sections were imaged using a BZ-9000 Keyence microscope.

Western blots and ELISA. Hearts were prepared for Western blots analysis as previously described (43). Briefly, heart tissues were mechanically homogenized by polytron (Kinematica) in ice-cold RIPA buffer consisting of Tris (pH 8.0) (50 mM; MilliporeSigma, catalog T1503), NaCl (150 mM; MilliporeSigma, catalog S7653), ethylene glycol tetraacetic acid (1 mM; MilliporeSigma, catalog E4884), NP-40 (1%; MilliporeSigma; catalog 3021), sodium deoxycholate (0.5%; MilliporeSigma, catalog D6750), SDS (0.1%; Bio-Rad, catalog 1610302), and protease inhibitors (MilliporeSigma, 05056489001), pH adjusted to 7.4. Heart homogenates were then centrifuged at 600 *g* for 5 minutes at 4°C to remove unbroken cells and debris. Protein quantification was performed on supernatants via bicinchoninic copper assay (MilliporeSigma, catalog C2284). Equal masses of protein were loaded in 4%–12% SDS page gels (Life Technologies, catalog NW04125BOX) and transferred to nitrocellulose membranes (VWR, catalog 27376-991). Anti-VEGF (Santa Cruz, catalog sc-152) and anti-GAPDH (Santa Cruz, catalog sc-137179) antibodies were diluted at a concentration of 1:1000 in blocking buffer consisting of 5% nonfat dry milk (Genessee, catalog 20-241) dissolved in TBS-T. HRP-conjugated goat anti-rabbit (Kirkegaard & Perry Laboratories, catalog 074-1516) and goat anti-mouse (Kirkegaard & Perry Laboratories, catalog 074-1806) secondary antibodies were diluted at a concentration of 1:3000 in blocking buffer. Chemiluminescent substrate (Bio-Rad, catalog 170-5061) was applied to membranes, and bands were imaged via Bio-Rad Chemidoc (Bio-Rad). Densitometry was performed using ImageJ software (NIH). Serum concentrations of BNP were measured by using a specific ELISA kit for BNP (MilliporeSigma, catalog RAB0386).

Cardiac MRI and measurement of cardiac function. MRI images were acquired at both the day before ISO injection, 5 weeks after LCWE injection, and the day before sacrifice. Each cohort was scanned via a 9.4 T Bruker's Biospin MRI system to assess ejection fraction. For each scan, a tripilot sequence from the Bruker's paravision system was implemented for the localization of the mouse heart. Next, several IntraGateFLASH sequences were performed for the left ventricle imaging. We then analyzed 5–6 sequential 1-mm slices in order to span the entire heart from bottom to top, with clear demonstration of ventricular dilation and contraction with a frame rate of 10 frames/s. To measure cardiac function, left ventricular chamber area outlined by the endocardial border for each slice at end diastole and end systole was mea-

sured. We calculated the left ventricular end-diastolic volume per slice at end-diastole (LV-EDV = ΣLV volume) and the left ventricular end-systolic volume per slice at end-systole (LV-ESV = ΣLV volume). Ejection fraction was calculated as (LV-EDV − LV-ESV)/LV-EEV × 100.

Statistics. Results are reported as mean ± SEM. All data were analyzed with the Graphpad Prism statistical program. Statistical significance was determined using the 2-tailed Student's *t* test (at 95% CI) to compare unpaired samples between experimental groups. A *P* value of less than 0.05 was considered statistically significant. For experiments involving 3 groups or more, we used 2-way ANOVA with the Tukey post hoc test. When the data analyzed were not distributed normally, we used the Mann-Whitney test (to compare unpaired samples between experimental groups).

Study approval. All animal experiments were performed under protocols that had been approved by the Institutional Animal Care and Use Committee at Cedars-Sinai Medical Center.

Author contributions

HHM, JS, M. Abe, and M. Arditi conceived the project and designed the experiments. HHM, JS, SC, MNR, and M. Abe performed the experiments. MCF helped perform the pathological analysis. RAG, TJL, and TRC helped with project conceptualization and manuscript writing. M. Abe, MNR, and M. Arditi wrote the manuscript with input from all authors.

Acknowledgments

We thank Ganghua Huang, Wenxuan Zhang, Malcom Lane, and Debbie Moreira for their technical support. We thank all the lab members for their helpful discussions. HHM was supported by NIH grant T32 AI089553; JS was supported by NIH grants T32 HL116273 and KL2 TR001882; MNR was supported by NIH grant R01 HL139766; SC was supported by NIH grant HL111483-01; and RAG was supported by NIH grant P01 HL112730. The MRI analysis was supported by the Cedars-Sinai Biomedical Imaging Research Institute seed grant to SC. The research was supported by NIH grant R01 AI072726 to M. Arditi.

Address correspondence to: Moshe Arditi, Cedars-Sinai Medical Center, 8700 Beverly Boulevard, Davis Building, Rooms D4024, 4025, 4027, Los Angeles, California 90048, USA. Phone: 310.423.4471; Email: moshe.arditi@cshs.org.

1. Kawasaki T, Kosaki F, Okawa S, Shigematsu I, Yanagawa H. A new infantile acute febrile mucocutaneous lymph node syndrome (MLNS) prevailing in Japan. *Pediatrics*. 1974;54(3):271–276.
2. Shulman ST, Rowley AH. Kawasaki disease: insights into pathogenesis and approaches to treatment. *Nat Rev Rheumatol*. 2015;11(8):475–482.
3. McCrindle BW, et al. Diagnosis, treatment, and long-term management of Kawasaki disease: a scientific statement for health professionals from the American Heart Association. *Circulation*. 2017;135(17):e927–e999.
4. Gordon JB, et al. The spectrum of cardiovascular lesions requiring intervention in adults after Kawasaki disease. *JACC Cardiovasc Interv*. 2016;9(7):687–696.
5. Gordon JB, Kahn AM, Burns JC. When children with Kawasaki disease grow up: Myocardial and vascular complications in adulthood. *J Am Coll Cardiol*. 2009;54(21):1911–1920.
6. Rizk SR, et al. Acute myocardial ischemia in adults secondary to missed Kawasaki disease in childhood. *Am J Cardiol*. 2015;115(4):423–427.
7. Daniels LB, Gordon JB, Burns JC. Kawasaki disease: late cardiovascular sequelae. *Curr Opin Cardiol*. 2012;27(6):572–577.
8. Burns JC, Capparelli EV, Brown JA, Newburger JW, Glode MP. Intravenous gamma-globulin treatment and retreatment in Kawasaki disease. US/Canadian Kawasaki Syndrome Study Group. *Pediatr Infect Dis J*. 1998;17(12):1144–1148.
9. Sundel RP, Burns JC, Baker A, Beiser AS, Newburger JW. Gamma globulin re-treatment in Kawasaki disease. *J Pediatr*. 1993;123(4):657–659.
10. Newburger JW, Takahashi M, Burns JC. Kawasaki disease. *J Am Coll Cardiol*. 2016;67(14):1738–1749.
11. Tremoulet AH, et al. Resistance to intravenous immunoglobulin in children with Kawasaki disease. *J Pediatr*. 2008;153(1):117–121.
12. Kato H, et al. Long-term consequences of Kawasaki disease. A 10- to 21-year follow-up study of 594 patients. *Circulation*. 1996;94(6):1379–1385.
13. Onouchi Z, et al. Long-term changes in coronary artery aneurysms in patients with Kawasaki disease: comparison of therapeutic regimens. *Circ J*. 2005;69(3):265–272.
14. Senzaki H. Long-term outcome of Kawasaki disease. *Circulation*. 2008;118(25):2763–2772.
15. Giacchi V, et al. Assessment of coronary artery intimal thickening in patients with a previous diagnosis of Kawasaki disease by using high resolution transthoracic echocardiography: our experience. *BMC Cardiovasc Disord*. 2014;14:106.
16. Holve TJ, Patel A, Chau Q, Marks AR, Meadows A, Zaroff JG. Long-term cardiovascular outcomes in survivors of Kawasaki disease. *Pediatrics*. 2014;133(2):e305–e311.
17. Shah V, et al. Cardiovascular status after Kawasaki disease in the UK. *Heart*. 2015;101(20):1646–1655.

18. Suzuki A, et al. Active remodeling of the coronary arterial lesions in the late phase of Kawasaki disease: immunohistochemical study. *Circulation*. 2000;101(25):2935–2941.
19. Burns JC, Shike H, Gordon JB, Malhotra A, Schoenwetter M, Kawasaki T. Sequelae of Kawasaki disease in adolescents and young adults. *J Am Coll Cardiol*. 1996;28(1):253–257.
20. Holman RC, Belay ED, Christensen KY, Folkema AM, Steiner CA, Schonberger LB. Hospitalizations for Kawasaki syndrome among children in the United States, 1997-2007. *Pediatr Infect Dis J*. 2010;29(6):483–488.
21. Burns JC. Kawasaki disease update. *Indian J Pediatr*. 2009;76(1):71–76.
22. Newburger JW, et al. Diagnosis, treatment, and long-term management of Kawasaki disease: a statement for health professionals from the Committee on Rheumatic Fever, Endocarditis and Kawasaki Disease, Council on Cardiovascular Disease in the Young, American Heart Association. *Circulation*. 2004;110(17):2747–2771.
23. Burns JC, Glodé MP. Kawasaki syndrome. *Lancet*. 2004;364(9433):533–544.
24. Orenstein JM, et al. Three linked vasculopathic processes characterize Kawasaki disease: a light and transmission electron microscopic study. *PLoS One*. 2012;7(6):e38998.
25. Liu AM, Ghazizadeh M, Onouchi Z, Asano G. Ultrastructural characteristics of myocardial and coronary microvascular lesions in Kawasaki disease. *Microvasc Res*. 1999;58(1):10–27.
26. Dionne A, Dahdah N. Myocarditis and Kawasaki disease. *Int J Rheum Dis*. 2018;21(1):45–49.
27. Fujiwara H, Hamashima Y. Pathology of the heart in Kawasaki disease. *Pediatrics*. 1978;61(1):100–107.
28. Harada M, et al. Histopathological characteristics of myocarditis in acute-phase Kawasaki disease. *Histopathology*. 2012;61(6):1156–1167.
29. Ayusawa MAO, Miyashita T. The study of death cases in acute phase Kawasaki disease over the last 10 years based on a National Survey [in Japanese]. *Pediatr Cardiol Cardiac Surg*. 2000;20:245.
30. Takahashi M. Myocarditis in Kawasaki syndrome. A minor villain? *Circulation*. 1989;79(6):1398–1400.
31. Printz BF, et al. Noncoronary cardiac abnormalities are associated with coronary artery dilation and with laboratory inflammatory markers in acute Kawasaki disease. *J Am Coll Cardiol*. 2011;57(1):86–92.
32. Frank B, et al. Myocardial strain and strain rate in Kawasaki disease: range, recovery, and relationship to systemic inflammation/coronary artery dilation. *J Clin Exp Cardiolog*. 2016;7(4):432.
33. Crystal MA, Syan SK, Yeung RS, Dipchand AI, McCrindle BW. Echocardiographic and electrocardiographic trends in children with acute Kawasaki disease. *Can J Cardiol*. 2008;24(10):776–780.
34. Tuan SH, et al. Cardiopulmonary function, exercise capacity, and echocardiography finding of pediatric patients with Kawasaki disease: an observational study. *Medicine (Baltimore)*. 2016;95(2):e2444.
35. Tuan SH, et al. Analysis of exercise capacity of children with Kawasaki disease by a coronary artery z score model (ZSP version 4) derived by the lambda-mu-sigma method. *J Pediatr*. 2018;201:128–133.
36. Dahdah N. Not just coronary arteritis, Kawasaki disease is a myocarditis, too. *J Am Coll Cardiol*. 2010;55(14):1507.
37. Nakamura Y, et al. Mortality among persons with a history of Kawasaki disease in Japan: mortality among males with cardiac sequelae is significantly higher than that of the general population. *Circ J*. 2008;72(1):134–138.
38. Lee Y, et al. Interleukin-1β is crucial for the induction of coronary artery inflammation in a mouse model of Kawasaki disease. *Circulation*. 2012;125(12):1542–1550.
39. Wakita D, et al. Role of interleukin-1 signaling in a mouse model of Kawasaki disease-associated abdominal aortic aneurysm. *Arterioscler Thromb Vasc Biol*. 2016;36(5):886–897.
40. Noval Rivas M, et al. CD8+ T cells contribute to the development of coronary arteritis in the Lactobacillus casei cell wall extract-induced murine model of Kawasaki disease. *Arthritis Rheumatol*. 2017;69(2):410–421.
41. de Lemos JA, McGuire DK, Drazner MH. B-type natriuretic peptide in cardiovascular disease. *Lancet*. 2003;362(9380):316–322.
42. Lee Y, et al. IL-1 signaling is critically required in stromal cells in Kawasaki disease vasculitis mouse model: role of both IL-1α and IL-1β. *Arterioscler Thromb Vasc Biol*. 2015;35(12):2605–2616.
43. Sin J, et al. The impact of juvenile coxsackievirus infection on cardiac progenitor cells and postnatal heart development. *PLoS Pathog*. 2014;10(7):e1004249.
44. de Couto G, et al. Macrophages mediate cardioprotective cellular postconditioning in acute myocardial infarction. *J Clin Invest*. 2015;125(8):3147–3162.
45. Ma Y, Mouton AJ, Lindsey ML. Cardiac macrophage biology in the steady-state heart, the aging heart, and following myocardial infarction. *Transl Res*. 2018;191:15–28.
46. Manlhiot C, Niedra E, McCrindle BW. Long-term management of Kawasaki disease: implications for the adult patient. *Pediatr Neonatol*. 2013;54(1):12–21.
47. Yagi S, et al. Two adults requiring implantable defibrillators because of ventricular tachycardia and left ventricular dysfunction caused by presumed Kawasaki disease. *Circ J*. 2005;69(7):870–874.
48. Kanegaye JT, et al. Recognition of a Kawasaki disease shock syndrome. *Pediatrics*. 2009;123(5):e783–e789.
49. Taddio A, et al. Describing Kawasaki shock syndrome: results from a retrospective study and literature review. *Clin Rheumatol*. 2017;36(1):223–228.
50. Yutani C, et al. Cardiac biopsy of Kawasaki disease. *Arch Pathol Lab Med*. 1981;105(9):470–473.
51. Yonesaka S, et al. Biopsy-proven myocardial sequels in Kawasaki disease with giant coronary aneurysms. *Cardiol Young*. 2010;20(6):602–609.
52. Matsuura H, et al. Gallium-67 myocardial imaging for the detection of myocarditis in the acute phase of Kawasaki disease (mucocutaneous lymph node syndrome): the usefulness of single photon emission computed tomography. *Br Heart J*. 1987;58(4):385–392.
53. Gordon JB, Burns JC. Management of sequelae of Kawasaki disease in adults. *Glob Cardiol Sci Pract*. 2017;2017(3):e201731.
54. Yonesaka S, et al. Endomyocardial biopsy in children with Kawasaki disease. *Acta Paediatr Jpn*. 1989;31(6):706–711.
55. Balakumar P, Singh AP, Singh M. Rodent models of heart failure. *J Pharmacol Toxicol Methods*. 2007;56(1):1–10.
56. Wang JJ, et al. Genetic dissection of cardiac remodeling in an isoproterenol-induced heart failure mouse model. *PLoS Genet*. 2016;12(7):e1006038.

57. Wallner M, et al. Acute catecholamine exposure causes reversible myocyte injury without cardiac regeneration. *Circ Res*. 2016;119(7):865–879.
58. Iemura M, Ishii M, Sugimura T, Akagi T, Kato H. Long term consequences of regressed coronary aneurysms after Kawasaki disease: vascular wall morphology and function. *Heart*. 2000;83(3):307–311.
59. Yamakawa R, et al. Coronary endothelial dysfunction after Kawasaki disease: evaluation by intracoronary injection of acetylcholine. *J Am Coll Cardiol*. 1998;31(5):1074–1080.
60. Hauser M, et al. Myocardial blood flow and coronary flow reserve in children with "normal" epicardial coronary arteries after the onset of Kawasaki disease assessed by positron emission tomography. *Pediatr Cardiol*. 2004;25(2):108–112.
61. Pinto FF, Laranjo S, Paramés F, Freitas I, Mota-Carmo M. Long-term evaluation of endothelial function in Kawasaki disease patients. *Cardiol Young*. 2013;23(4):517–522.
62. Dhillon R, et al. Endothelial dysfunction late after Kawasaki disease. *Circulation*. 1996;94(9):2103–2106.
63. Furuyama H, et al. Altered myocardial flow reserve and endothelial function late after Kawasaki disease. *J Pediatr*. 2003;142(2):149–154.
64. McCrindle BW, McIntyre S, Kim C, Lin T, Adeli K. Are patients after Kawasaki disease at increased risk for accelerated atherosclerosis? *J Pediatr*. 2007;151(3):244–248.e1.
65. Selamet Tierney ES, et al. Vascular health in Kawasaki disease. *J Am Coll Cardiol*. 2013;62(12):1114–1121.
66. Gupta-Malhotra M, et al. Atherosclerosis in survivors of Kawasaki disease. *J Pediatr*. 2009;155(4):572–577.
67. Gravel H, Curnier D, Dallaire F, Fournier A, Portman M, Dahdah N. Cardiovascular response to exercise testing in children and adolescents late after Kawasaki disease according to coronary condition upon onset. *Pediatr Cardiol*. 2015;36(7):1458–1464.
68. Shimizu C, et al. Cardiovascular pathology in 2 young adults with sudden, unexpected death due to coronary aneurysms from Kawasaki disease in childhood. *Cardiovasc Pathol*. 2015;24(5):310–316.
69. Yutani C, et al. Histopathological study on right endomyocardial biopsy of Kawasaki disease. *Br Heart J*. 1980;43(5):589–592.
70. Tremoulet AH, et al. Rationale and study design for a phase I/IIa trial of anakinra in children with Kawasaki disease and early coronary artery abnormalities (the ANAKID trial). *Contemp Clin Trials*. 2016;48:70–75.
71. Burns JC, Kone-Paut I, Kuijpers T, Shimizu C, Tremoulet A, Arditi M. Review: Found in translation: international initiatives pursuing interleukin-1 blockade for treatment of acute Kawasaki disease. *Arthritis Rheumatol*. 2017;69(2):268–276.
72. Dubois M, Gilles KA, Hamilton JK, Rebers PA, Smith F. Colorimetric method for determination of sugars and related substances. *Anal Chem*. 1956;28(3):350–356.